

Supplementary Material

Paper-based electrochemical biosensors for voltammetric detection of miRNA biomarkers using reduced graphene oxide or MoS₂ nanosheets decorated with gold nanoparticle electrodes

Hilal Torul ^{1,a}, Ece Yarali ^{2,a}, Ece Eksin ^{2,a}, Abhijit Ganguly ³, John Benson ⁴, Ugur Tamer ^{1,*}, Pagona Papakonstantinou ^{3,*} and Arzum Erdem ^{2,*}

¹ Department of Analytical Chemistry, Faculty of Pharmacy, Gazi University, 06330 Ankara, Turkey

² Department of Analytical Chemistry, Faculty of Pharmacy, Ege University, 35100 Bornova, Turkey

³ School of Engineering, Engineering Research Institute, Ulster University, Newtownabbey BT37 0QB, United Kingdom

⁴ 2-DTech, Core Technology Facility, 46 Grafton Street, Manchester M13 9NT, United Kingdom

Corresponding Authors:

E-mail addresses: arzum.erdem@ege.edu.tr (A. Erdem), p.papakonstantinou@ulster.ac.uk (P.

Papakonstantinou), utamer@gazi.edu.tr (U. Tamer)

miRNAs and the base sequences of all oligonucleotides:

miRNA-155, miRNA-21 specific DNA probe, their synthetic target miRNA-155 or miRNA-21 and the other oligonucleotides; non-complementary RNA target, the oligonucleotides having a single base were obtained from (as lyophilized powder) TIB Molbiol (Germany). miRNAs and the base sequences of all oligonucleotides were listed below:

thiol link miRNA-155 specific DNA probe (Probe-1)

5'- SH-ACC CCT ATC ACG ATT AGC ATT AA-3'

miRNA-155 RNA target

5'- UUA AUG CUA AUC GUG AUA GGG GU-3'

miRNA-155 non-complementary sequence (NC)

5'-UGG CAG UGU CUU AGC UGG UUG U-3'

miRNA-155 mismatch sequence (MM)

5'-UUA AUG CUA AUC GUC AUA GGG GU-3'

thiol link miRNA-21 specific DNA probe (Probe-2)

5'- SH-TCA ACA TCA GTC TGA TAA GCT A-3'

miRNA-21 RNA target

5'- UAG CUU AUC AGA CUG AUG UUG A-3'

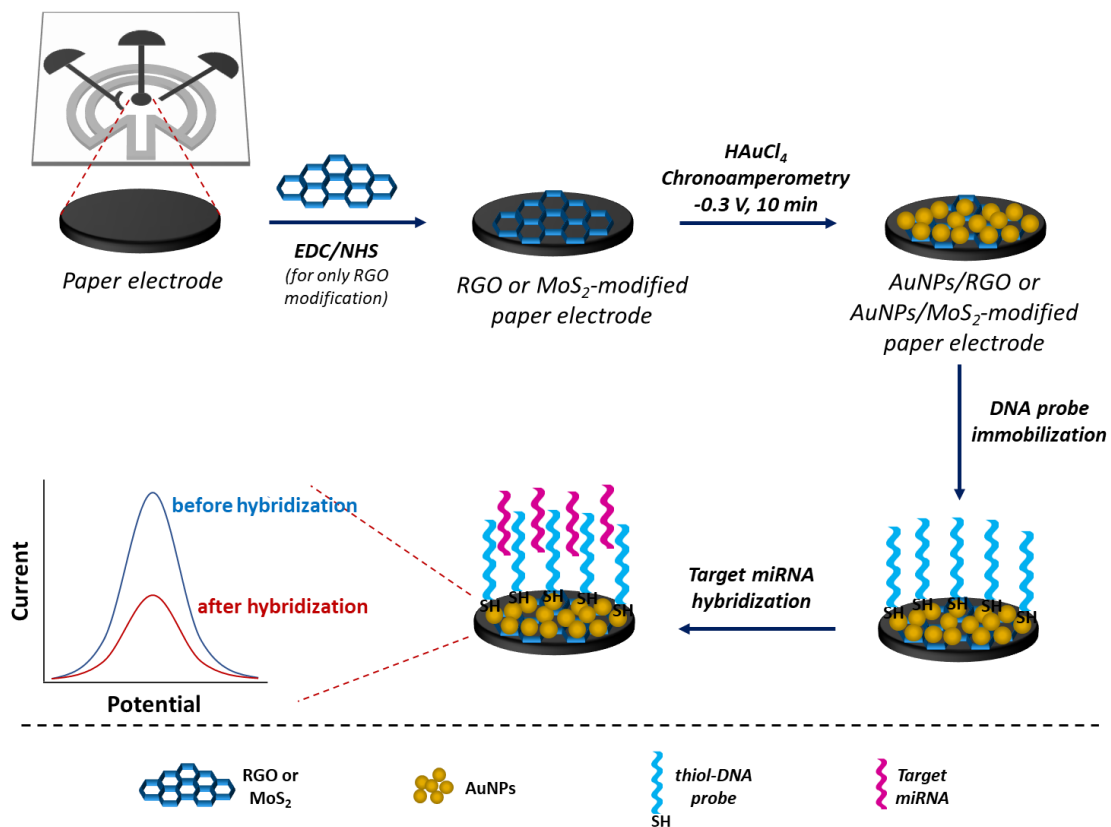
miRNA-21 non-complementary sequence (NC)

5'- AUG CAU GCA UGC AUG CAU GCA A-3'

miRNA-21 mismatch sequence (MM)

5'-UAG CUU AUC AGA CUC AUG UUG A-3'

The stock solutions of DNA probe and miRNA target were prepared in Tris-EDTA buffer (pH 8.00) and stored in freezer. The stock solutions were diluted using PBS (pH 7.40) solution.



Scheme S1. The schematic illustration of RGO/MoS₂-modified paper electrode assembly fabrication and Probe/miRNA assembling

Results obtained by AuNPs/RGO-modified paper electrode

The electrochemical characterization of RGO-modified paper electrode

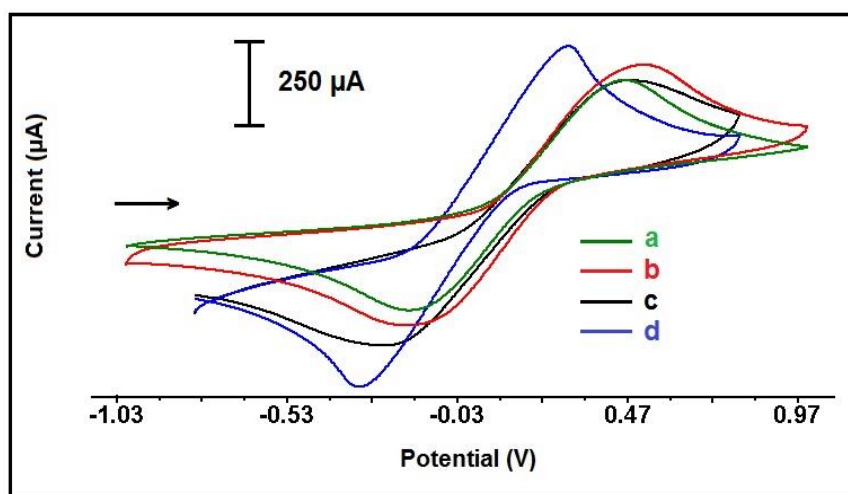


Figure S1. CVs recorded in optimum conditions by using (a) unmodified paper electrode, (b) RGO-modified paper electrode, (c) after activation of RGO-modified paper electrode using covalent agents, (d) after electrodeposition of AuNPs onto the surface of chemically activated and RGO-modified paper electrode in the presence of 50.0 mM potassium ferricyanide in 100.0 mM KCl.

Table S1. The anodic current I_a (μA) and the cathodic current I_c (μA), the relative charge, Q_a and Q_c of $[\text{Fe}(\text{CN})_6]^{3-/4-}$ measured by unmodified, RGO modified, after activation of RGO-modified paper electrode using covalent agents and AuNPs/RGO-modified paper electrode.

| | I_a (μA) | I_c (μA) | Q_a (mC) | Q_c (mC) | A (cm^2) |
|---|-------------------------|-------------------------|------------|------------|-----------------------|
| Unmodified paper electrode | 240 | 281 | 2.17 | 3.80 | 0.020 |
| RGO-modified paper electrode | 305.9 | 347.9 | 3.3 | 4.41 | 0.026 |
| after activation of RGO-modified paper electrode using covalent agents | 211.3 | 296.5 | 2.23 | 4.97 | 0.018 |
| AuNPs/RGO-modified paper electrode | 425.6 | 406 | 2.53 | 4.87 | 0.036 |

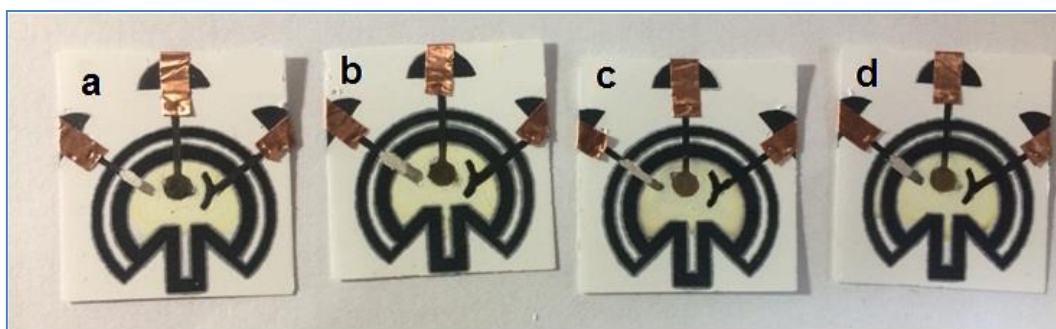


Figure S2. The images of (a) 2.5 mM, (b) 5.0 mM, (c) 10.0 mM, (d) 15.0 mM HAuCl₄ deposited RGO-modified paper electrode

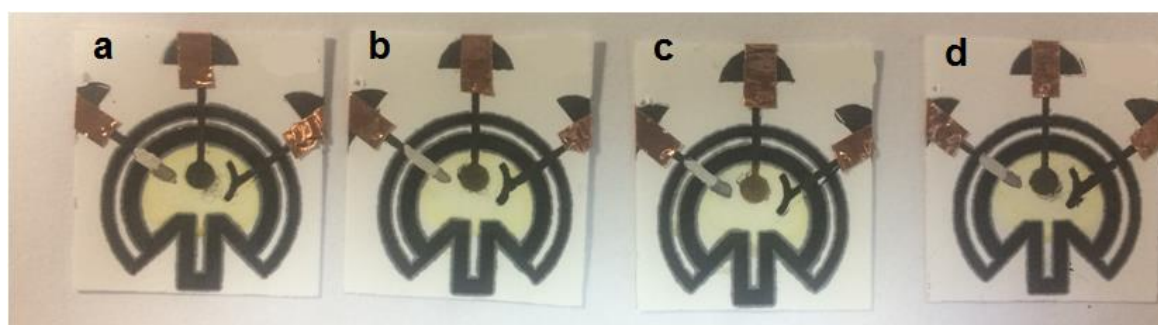


Figure S3. The images of AuNPs/RGO-modified paper electrode after deposition of 5.0 mM HAuCl₄ during (a) 5 min, (b) 7 min, (c) 10 min, (d) 15 min.

The effect of probe concentration at hybridization process

The effect of DNA probe concentration upon the hybridization was investigated (Fig. S4). The nucleic acid hybridization was performed between 2.0 $\mu\text{g/mL}$ miRNA-155 target and its DNA probe (Probe-1) at different concentration level from 0.5, 1.0 and 2.0 $\mu\text{g/mL}$. After immobilization of 0.5 $\mu\text{g/mL}$ Probe-1, the average oxidation signal of $[\text{Fe}(\text{CN})_6]^{3-/4-}$ was measured as $32.43 \pm 1.12 \mu\text{A}$ (RSD%, 3.47%, n=3). According to the signal measured in the absence of Probe-1, the highest decrease was obtained in the presence of 0.5 $\mu\text{g/mL}$ Probe-1 as 25.9% and measured as $24.01 \pm 6.97 \mu\text{A}$ (RSD%, 29.01%, n=3). Therefore, 0.5 $\mu\text{g/mL}$ Probe-1 concentration was determined as optimum for further studies.

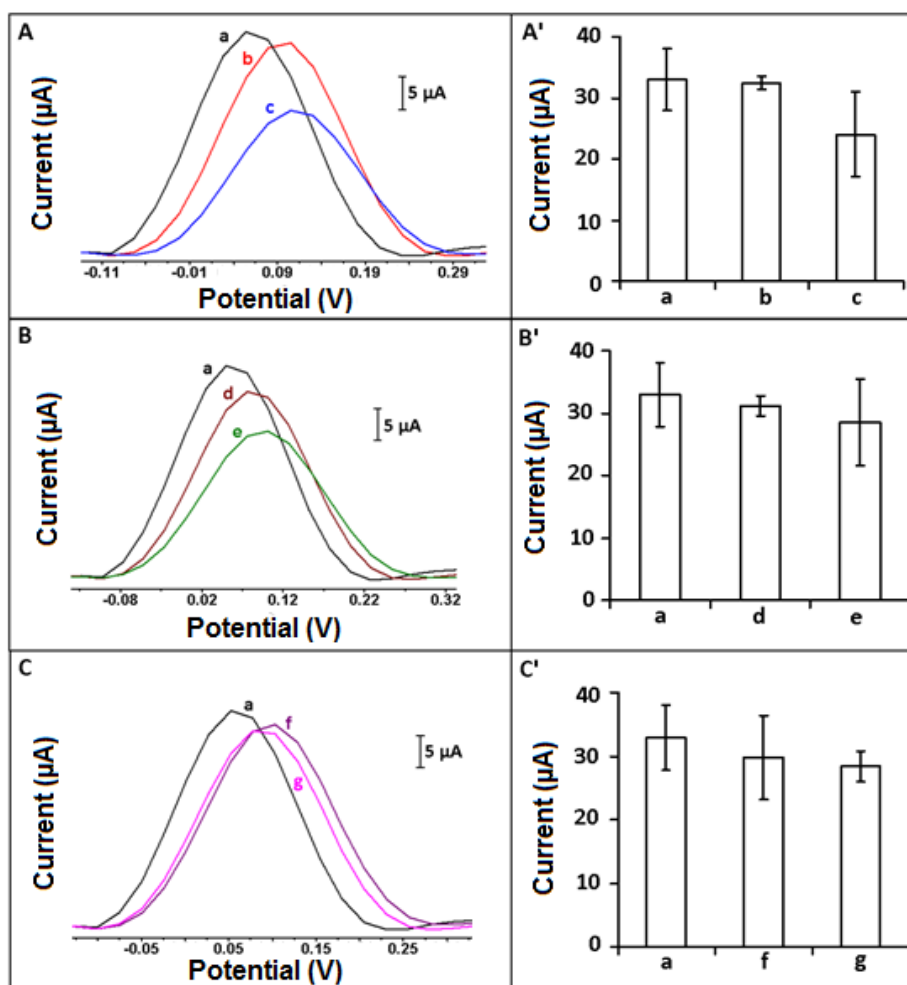


Figure S4. (A) DPVs (A') histograms representing (a) AuNPs/RGO-modified paper electrode, (b) 0.5 $\mu\text{g/mL}$ Probe-1 immobilized AuNPs/RGO-modified paper electrode, after hybridization of 0.5 $\mu\text{g/mL}$ miRNA 155 Probe-1 with (c) 2.0 $\mu\text{g/mL}$ miRNA-155 target ($n=2$). (B) DPVs (B') histograms representing (d) 1.0 $\mu\text{g/mL}$ miRNA 155 Probe-1 immobilized AuNPs/RGO-modified paper electrode, after hybridization of 1.0 $\mu\text{g/mL}$ Probe-1 with (e) 2.0 $\mu\text{g/mL}$ miRNA-155 target ($n=2$). (C) DPVs (C') histograms representing (f) 2.0 $\mu\text{g/mL}$ Probe-1 immobilized AuNPs/RGO-modified paper electrode, after hybridization of 2.0 $\mu\text{g/mL}$ Probe-1 with (g) 2.0 $\mu\text{g/mL}$ miRNA-155 target ($n=2$).

The effect of probe immobilization time onto the electrode surface upon the hybridization process

For the optimization of probe immobilization time, a short period (i.e. 10 min) which was used in our previous work [35] in contrast to a longer period (i.e. 30 min) were tested. Since the electrode surface dried over 30 min, there is no need to examine a much longer immobilization time in our study.

In the absence of Probe-1, the oxidation signal of $[\text{Fe}(\text{CN})_6]^{3-/4-}$ was measured as $32.96 \pm 5.12 \mu\text{A}$ by AuNPs/RGO-modified paper electrode. The average oxidation signal of $[\text{Fe}(\text{CN})_6]^{3-/4-}$ was measured as $32.43 \pm 1.12 \mu\text{A}$ (RSD%, 3.47%, $n=3$) and $25.60 \pm 0.14 \mu\text{A}$ (RSD%, 0.55%, $n=3$) after immobilization of 0.5 $\mu\text{g/mL}$ Probe-1 during 10 and 30 min, respectively (Fig. S5). According to the signal measured in the absence of Probe-1, the highest decrease at the oxidation signal was obtained in the case of 30

min Probe-1 immobilization as 22 % (Table S2). Thus, 30 min was chosen as optimum probe immobilization time for our further studies.

Table S2. The oxidation signal of $[\text{Fe}(\text{CN})_6]^{3-/4-}$ measured before/after 0.5 $\mu\text{g}/\text{mL}$ DNA probe immobilization onto the surface of AuNPs/RGO-modified paper electrode during 10 and 30 min and HE% values.

| | | I (μA) | HE% |
|------------------------------------|----|---------------------|------|
| AuNPs/RGO-modified paper electrode | | 32.96 ± 5.12 | |
| Probe-1 immobilization time (min) | 10 | 32.43 ± 1.12 | 1.6% |
| | 30 | 25.60 ± 0.14 | 22% |

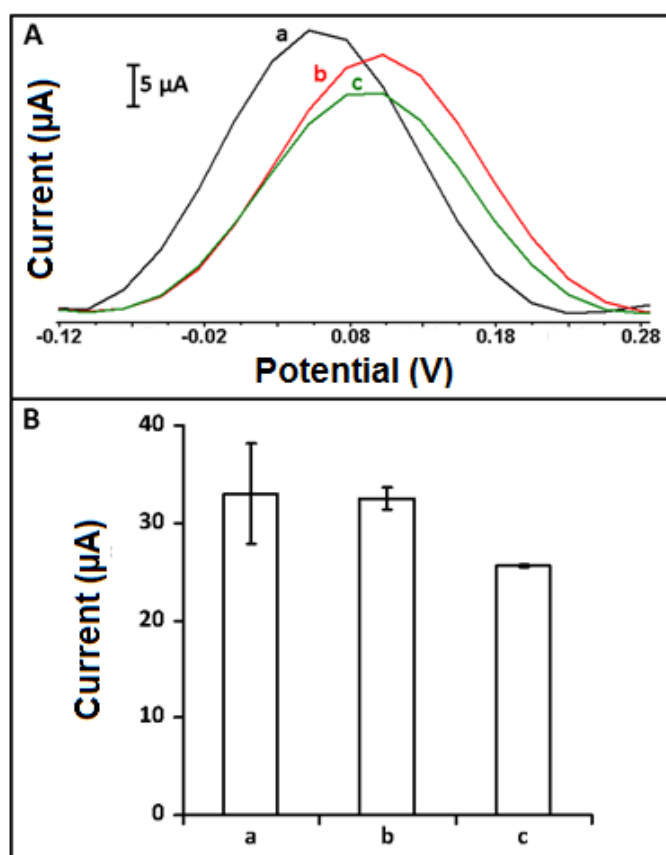


Figure S5. (A) DPVs (B) histograms representing 1.0 mM $[\text{Fe}(\text{CN})_6]^{3-/4-}$ oxidation signal obtained by (a) AuNPs/RGO-modified paper electrode, after immobilization of 0.5 $\mu\text{g}/\text{mL}$ Probe-1 during (b) 10 min (c) 30 min onto the surface of AuNPs/RGO-modified paper electrode ($n=3$).

The effect of hybridization time upon the hybridization process

For the optimization of hybridization time, a short (i.e. 5 min) which was used in our previous work [35], in contrast to a longer period (i.e. 15 min) were tested.

The hybridization of 0.5 $\mu\text{g}/\text{mL}$ Probe-1 and 1.0 $\mu\text{g}/\text{mL}$ miRNA-155 target was done during 5 and 15 min (Fig. S6). The average oxidation signal of $[\text{Fe}(\text{CN})_6]^{3-/4-}$ was measured as $16.70 \pm 4.17 \mu\text{A}$ (RSD%,

24.98%, n=4) and $20.36 \pm 10.68 \mu\text{A}$ (RSD%, 52.46%, n=4) after hybridization of Probe-1 with miRNA-155 target during 5 min and 15 min, respectively. According to the signal measured in the absence of target, the highest decrease (28.9%) was recorded in the case of 5 min hybridization time. Thus, it was chosen as optimum hybridization time for further studies.

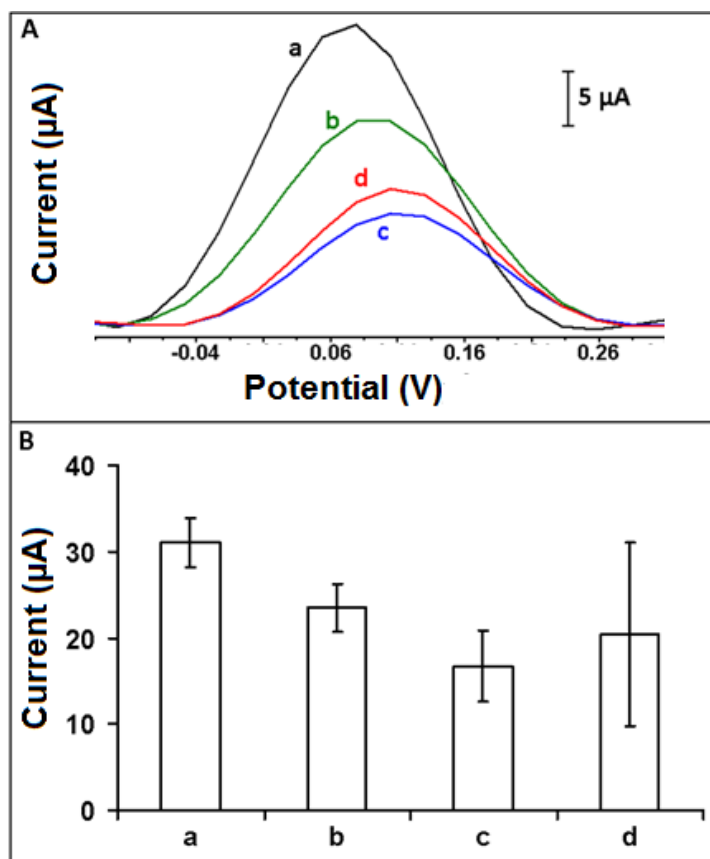


Figure S6. (A) DPVs, (B) histograms representing the $[\text{Fe}(\text{CN})_6]^{3-/4-}$ oxidation signal obtained by (a) AuNPs/RGO-modified paper electrode, (b) 0.5 $\mu\text{g}/\text{mL}$ Probe-1 immobilized AuNPs/RGO-modified paper electrode, after the hybridization of Probe-1 with miRNA-155 target during (c) 5 min, (d) 15 min (n=4).

Table S3. The oxidation signal of $[\text{Fe}(\text{CN})_6]^{3-/4-}$ measured before/after hybridization of Probe-1 and miRNA-155 target in its different concentrations (n=3) and HE% values.

| | | I (μA) | |
|---|------|---------------------|------------|
| Probe-1 immobilized AuNPs/RGO-modified paper electrode | | 26.79 ± 2.42 | HE% |
| [miRNA-155] ($\mu\text{g}/\text{mL}$) | 0.25 | 24.69 ± 0.34 | 7.8% |
| | 0.5 | 22.34 ± 3.06 | 16.6% |
| | 0.75 | 18.01 ± 0.20 | 32.7% |
| | 1 | 16.83 ± 1.91 | 37.1% |
| | 1.5 | 16.94 ± 0.76 | 36.7% |
| | 2 | 17.25 ± 0.95 | 35.6% |

Table S4. The oxidation signal of $[\text{Fe}(\text{CN})_6]^{3-/4-}$ and decrease % at the signal after hybridization of Probe-2 and miRNA-21 target in its different concentrations (n=3).

| | | I (μA) | |
|---|------|---------------------|------------|
| Probe-2 immobilized AuNPs/RGO-modified paper electrode | | 29.70 \pm 0.20 | HE% |
| [miRNA-21] ($\mu\text{g/mL}$) | 0.25 | 27.36 \pm 3.59 | 7.8% |
| | 0.5 | 23.40 \pm 2.96 | 21.2% |
| | 0.75 | 20.73 \pm 2.34 | 30.2% |
| | 1 | 16.85 \pm 1.09 | 43.2% |
| | 1.5 | 17.22 \pm 0.65 | 42.0% |
| | 2 | 17.16 \pm 0.08 | 42.2% |

Selectivity of the assay on voltammetric detection of miRNA-155 by AuNPs/RGO-modified paper electrode

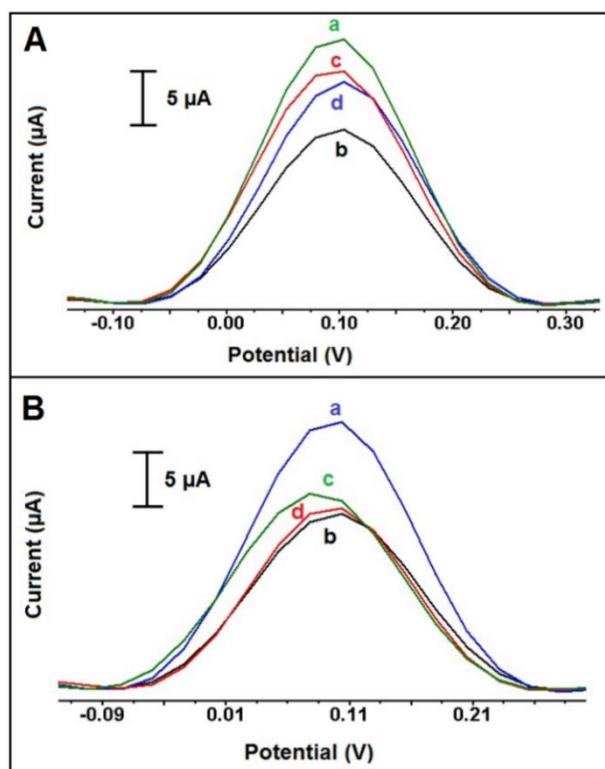


Figure S7. (A) Voltammograms representing the $[\text{Fe}(\text{CN})_6]^{3-/4-}$ oxidation signal obtained by (a) Probe-1 immobilized AuNPs/RGO-modified paper electrode in the absence of miRNA-155 target, after hybridization of Probe-1 with (b) miRNA-155 target, (c) NC, and (d) MM, individually. (B) Voltammograms representing the $[\text{Fe}(\text{CN})_6]^{3-/4-}$ oxidation signal obtained by (a) Probe-2 immobilized AuNPs/RGO-modified paper electrode in the absence of miRNA-155 target, after hybridization of

Probe-1 (b) with only miRNA-155 target, (c) in target:NC (1:1) mixture, and (d) in target:MM (1:1) mixture.

Table S5. The average $[\text{Fe}(\text{CN})_6]^{3-/4-}$ oxidation signals measured before and after hybridization of Probe-1 with miRNA-155 target, NC, MM, the mixture sample containing target:NC (1:1) or the mixture sample containing target:MM (1:1). HE% calculated according to the oxidation signals obtained after hybridization.

| | I (μA) | |
|---|-------------------------------------|------------|
| Probe-1 immobilized AuNPs/RGO-modified paper electrode | $29.47 \pm 0.44 \mu\text{A}$ | HE% |
| miRNA-155 target | $17.32 \pm 3.22 \mu\text{A}$ | 41.2% |
| NC | $20.05 \pm 2.35 \mu\text{A}$ | 31.9% |
| MM | $20.04 \pm 2.71 \mu\text{A}$ | 31.9% |
| miRNA-155 target:NC (1:1) mixture | $18.40 \pm 1.62 \mu\text{A}$ | 37.5% |
| miRNA-155 target:MM (1:1) mixture | $21.67 \pm 5.12 \mu\text{A}$ | 26.4% |

Selectivity of the assay on voltammetric detection of miRNA-21 by AuNPs/RGO-modified paper electrode

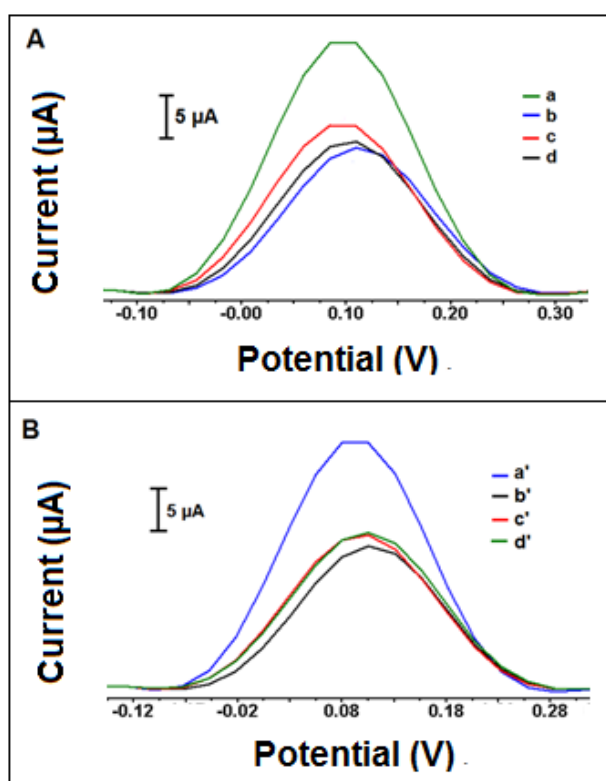


Figure S8. (A) Voltammograms representing the $[\text{Fe}(\text{CN})_6]^{3-/4-}$ oxidation signal obtained by (a) Probe-2 immobilized AuNPs/RGO-modified paper electrode in the absence of miRNA-21 target, after hybridization of Probe-2 with (b) miRNA-21 target, (c) NC, and (d) MM, individually. (B) Voltammograms representing the $[\text{Fe}(\text{CN})_6]^{3-/4-}$ oxidation signal obtained by (a') Probe-2 immobilized AuNPs/RGO-modified paper electrode in the absence of miRNA-21 target, after hybridization of Probe-2 (b') with only miRNA-21 target, (c') in target:NC (1:1) mixture, and (d') in target:MM (1:1) mixture

Table S6. The average $[\text{Fe}(\text{CN})_6]^{3-/4-}$ oxidation signals measured before and after hybridization of Probe-2 with miRNA-21 target, NC, MM, the mixture sample containing target:NC (1:1) or the mixture sample containing target:MM (1:1). HE % calculated according to the oxidation signals obtained after hybridization.

| | I (μA) | HE% |
|---|------------------------------|-------|
| Probe-2 immobilized AuNPs/RGO-modified paper electrode | $25.83 \pm 5.08 \mu\text{A}$ | |
| miRNA-21 target | $17.00 \pm 3.17 \mu\text{A}$ | 34.1% |
| NC | $20.64 \pm 5.75 \mu\text{A}$ | 20.1% |
| MM | $18.65 \pm 4.12 \mu\text{A}$ | 27.8% |
| miRNA-21 target:NC (1:1) mixture | $17.65 \pm 4.09 \mu\text{A}$ | 31.7% |
| miRNA-21 target:MM (1:1) mixture | $18.44 \pm 4.09 \mu\text{A}$ | 28.6% |

Results obtained by AuNPs/MoS₂-modified paper electrode

The electrochemical characterization of AuNPs/MoS₂-modified paper electrode

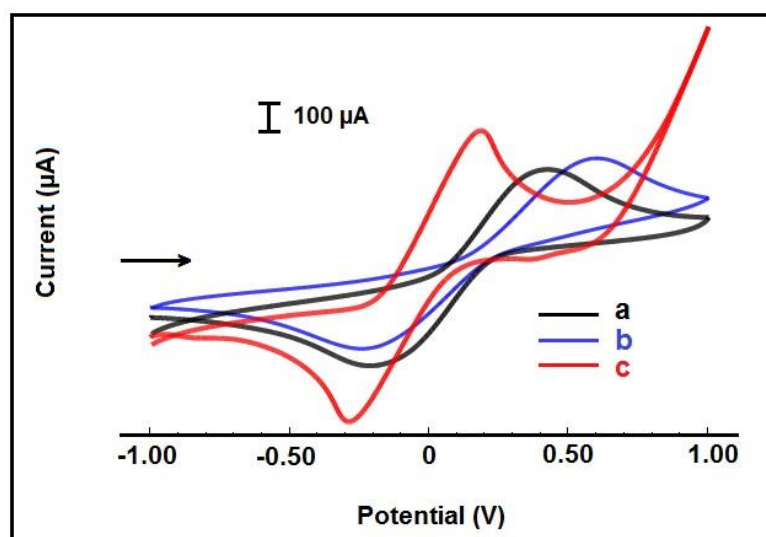


Figure S9. CVs recorded in optimum conditions by (a) unmodified paper electrode, (b) MoS₂-modified paper electrode, (c) AuNPs electrodeposited MoS₂-modified paper electrodes in the presence of 50.0 mM potassium ferricyanide in 100.0 mM KCl.

Table S7. The anodic current I_a (μA) and the cathodic current I_c (μA), the relative charge, Q_a and Q_c of $[\text{Fe}(\text{CN})_6]^{3-/4-}$ measured by unmodified, MoS_2 modified and AuNPs/ MoS_2 -modified paper electrode.

| | I_a (μA) | I_c (μA) | Q_a (mC) | Q_c (mC) | A (cm^2) |
|---|--|--|------------------------------|------------------------------|--|
| Unmodified paper electrode | 236.15 | 241.36 | 2.23 | 3.10 | 0.020 |
| MoS_2-modified paper electrode | 245.23 | 280.60 | 2.21 | 3.91 | 0.021 |
| AuNPs/MoS_2-modified paper electrode | 415.77 | 448.02 | 4.40 | 4.91 | 0.035 |

The effect of probe concentration at hybridization process:

The effect of DNA probe concentration upon the hybridization was investigated (Fig. S10). The nucleic acid hybridization was performed between $1.0 \mu\text{g/mL}$ miRNA-155 target and its Probe-1 at the different concentration level from 0.5, and $1.0 \mu\text{g/mL}$ onto the surface of AuNPs/ MoS_2 -modified paper electrode. After immobilization of $0.5 \mu\text{g/mL}$ Probe-1, the average oxidation signal of $[\text{Fe}(\text{CN})_6]^{3-/4-}$ was measured as $28.39 \pm 0.94 \mu\text{A}$ (RSD%, 3.32%, $n=5$), whereas the oxidation signal was measured as $32.06 \pm 0.76 \mu\text{A}$ (RSD%, 2.36%, $n=3$) after immobilization of $1.0 \mu\text{g/mL}$ Probe-1. After hybridization of $0.5 \mu\text{g/mL}$ or $1.0 \mu\text{g/mL}$ Probe-1 with miRNA-155 target the oxidation signals were measured as $22.61 \pm 0.62 \mu\text{A}$ (RSD%, 2.74%, $n=3$) and $24.59 \pm 2.79 \mu\text{A}$ (RSD%, 11.35%, $n=3$), respectively. According to the more reproducible results, $0.5 \mu\text{g/mL}$ Probe-1 concentration was determined as optimum for further studies.

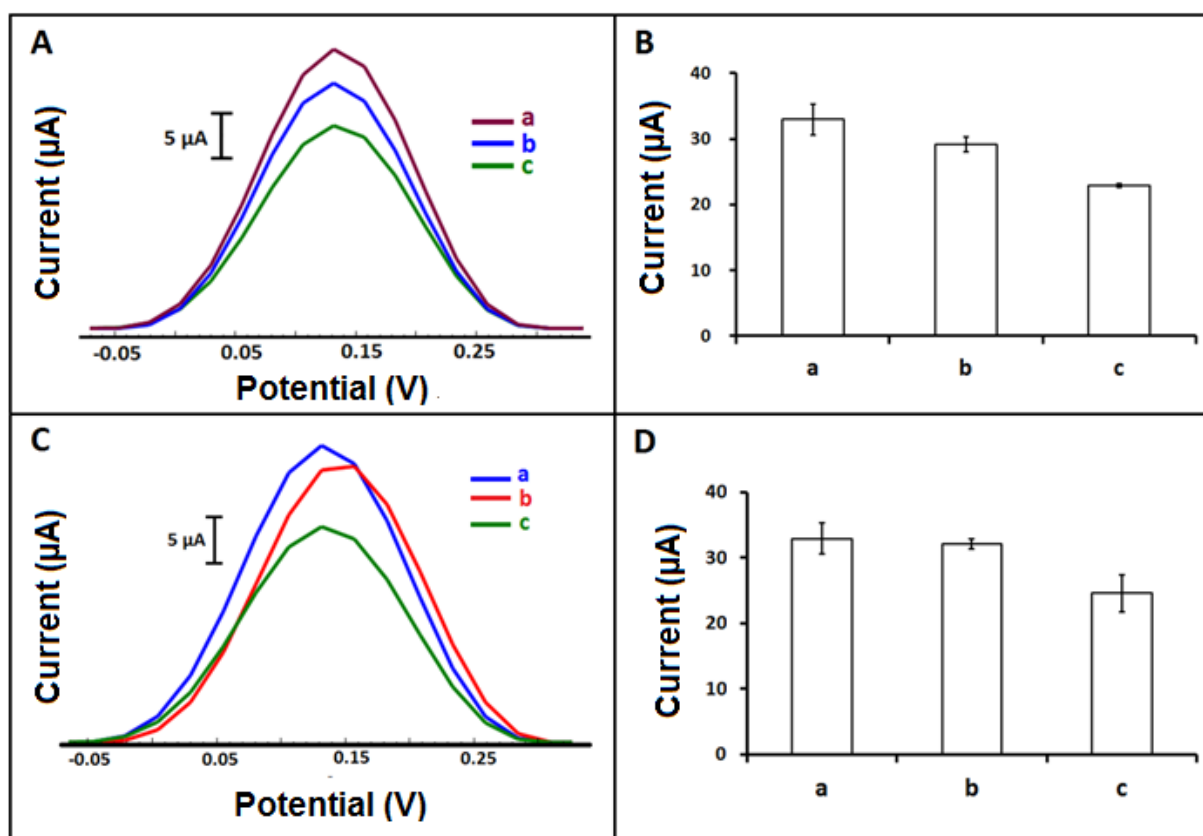


Figure S10. (A) DPVs (B) histograms representing (a) AuNPs/MoS₂-modified paper electrode, (b) 0.5 μg/mL DNA probe immobilized AuNPs/MoS₂-modified paper electrode, (c) after hybridization of 0.5 μg/mL DNA probe with 1.0 μg/mL miRNA-155 target (n=2). (C) DPVs (D) histograms representing (a) AuNPs/MoS₂-modified paper electrode, (b) 1.0 μg/mL DNA probe immobilized AuNPs/MoS₂-modified paper electrode, (c) after hybridization of 1.0 μg/mL DNA probe with 1.0 μg/mL miRNA-155 target (n=2).

The effect of hybridization time upon the hybridization process

The hybridization of 0.5 μg/mL Probe-1 and 1.0 μg/mL miRNA-155 target was done during 5 and 15 min hybridization time (Fig. S11). The average oxidation signal of [Fe(CN)₆]^{3-/4-} was measured as 22.95 ± 0.30 μA (RSD%, 1.33%, n=2) and 30.55 ± 7.40 μA (RSD%, 24.24%, n=3) after hybridization of Probe-1 with miRNA-155 target during 5 min and 15 min, respectively. According to the signal obtained in the absence of target, the highest decrease as 32% was obtained in case of 5 min hybridization time. Thus, 5 min hybridization time was chosen as optimum for further studies.

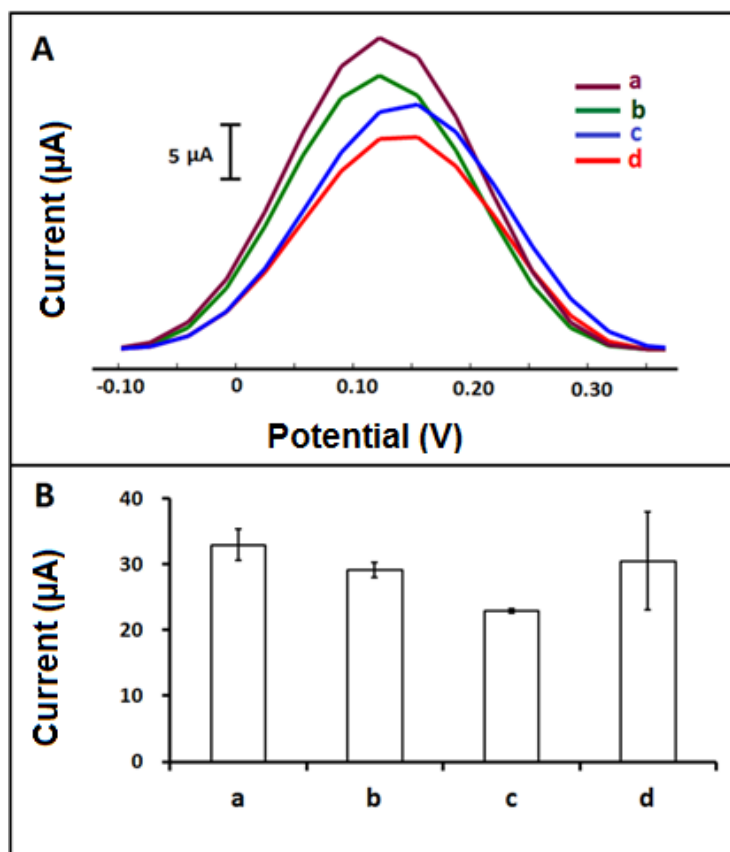


Figure S11. (A) DPVs, (B) histograms representing the $[\text{Fe}(\text{CN})_6]^{3-/4-}$ oxidation signal obtained by (a) AuNPs/MoS₂-modified paper electrode, (b) 0.5 $\mu\text{g/mL}$ Probe-1 immobilized AuNPs/MoS₂-modified paper electrode, after the hybridization of Probe-1 with miRNA-155 target during (c) 5 min, (d) 15 min (n=3).

Voltammetric detection of miRNA-21 by AuNPs and MoS₂-modified paper electrode

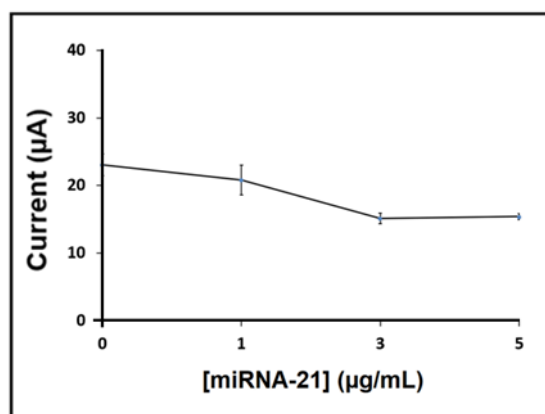


Figure S12. The line graph based on the average $[\text{Fe}(\text{CN})_6]^{3-/4-}$ oxidation signal measured after hybridization between Probe-2 and miRNA-21 target with its various concentrations from 0 to 5.0 $\mu\text{g/mL}$ (n=3).

Table S8. The oxidation signal of $[\text{Fe}(\text{CN})_6]^{3-/4-}$ and HE% values that calculated after hybridization of Probe-2 and miRNA-21 target in its different concentrations (n=3).

| | | I (μA) | HE% |
|---|-----|---------------------|-------|
| Probe-2 immobilized AuNPs/MoS₂-modified paper electrode | | 23.06 \pm 1.59 | |
| [miRNA-21] ($\mu\text{g/mL}$) | 0.5 | 22.48 \pm 1.62 | 2.5% |
| | 1 | 20.80 \pm 2.21 | 9.8% |
| | 1.5 | 19.14 \pm 1.92 | 16.9% |
| | 2 | 17.35 \pm 0.65 | 24.7% |
| | 2.5 | 16.69 \pm 0.92 | 27.6% |
| | 3 | 15.13 \pm 0.76 | 34.3% |
| | 5 | 15.38 \pm 0.45 | 33.3% |

Voltammetric detection of miRNA-155 by AuNPs and MoS₂-modified paper electrode

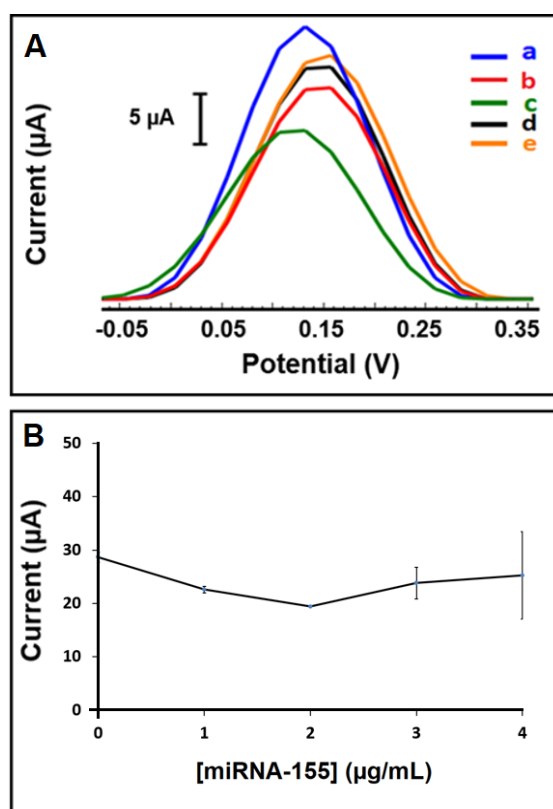


Figure S13. (A) Voltammograms representing the $[\text{Fe}(\text{CN})_6]^{3-/4-}$ oxidation signals obtained by (a) Probe-1 immobilized AuNPs/MoS₂-paper electrode, after hybridization of Probe-1 with miRNA-155 target at the concentrations of (b) 1.0 $\mu\text{g/mL}$, (c) 2.0 $\mu\text{g/mL}$, (d) 3.0 $\mu\text{g/mL}$, (e) 4.0 $\mu\text{g/mL}$. (B) The line graph based on the average $[\text{Fe}(\text{CN})_6]^{3-/4-}$ oxidation signal after hybridization between Probe-1 and miRNA-155 target with its various concentrations from 0 to 4.0 $\mu\text{g/mL}$ (n=3).

Table S9. The oxidation signal of $[\text{Fe}(\text{CN})_6]^{3-/4-}$ and HE% values that calculated after hybridization of Probe-1 and miRNA-155 target in its different concentrations (n=3).

| | | I (μA) | |
|---|---|---------------------|------------|
| Probe-1 immobilized AuNPs/MoS₂-modified paper electrode | | 28.65 \pm 0.94 | HE% |
| [miRNA-155] ($\mu\text{g/mL}$) | 1 | 22.61 \pm 0.62 | 21.0% |
| | 2 | 19.38 \pm 0.04 | 32.3% |
| | 3 | 23.80 \pm 2.98 | 16.9% |
| | 4 | 25.24 \pm 8.17 | 11.9% |

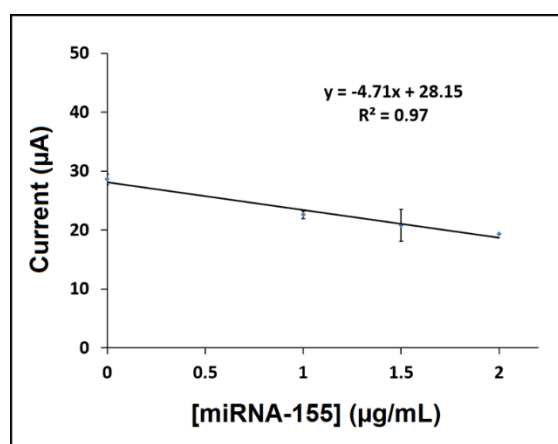


Figure S14. The calibration plot obtained after hybridization between Probe-1 and miRNA-155 target with its various concentrations from 0 to 2.0 $\mu\text{g/mL}$ (n=3).

Selectivity of the assay on voltammetric detection of miRNA-155 by AuNPs and MoS₂-modified paper electrode

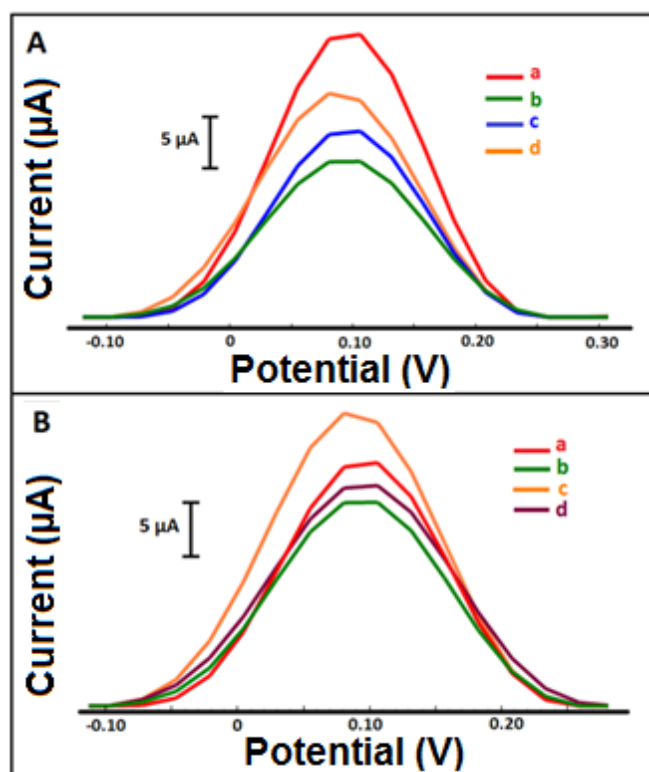


Figure S15. (A) Voltammograms representing the $[\text{Fe}(\text{CN})_6]^{3-/4-}$ oxidation signal obtained by (a) Probe-1 immobilized AuNPs/MoS₂-modified paper electrode in the absence of miRNA-155 target, after hybridization of Probe-1 with (b) miRNA-155 target, (c) NC, and (d) MM, individually. (B) Voltammograms representing the $[\text{Fe}(\text{CN})_6]^{3-/4-}$ oxidation signal obtained by (a) Probe-1 immobilized AuNPs/MoS₂-modified paper electrode in the absence of miRNA-155 target, after hybridization of Probe-1 (b) with only miRNA-155 target, (c) in target:NC (1:1) mixture, and (d) in target:MM (1:1) mixture.

Table S10. The average $[\text{Fe}(\text{CN})_6]^{3-/4-}$ oxidation signals (n=2) measured before and after hybridization of Probe-1 with miRNA-155 target, NC, MM, the mixture sample containing target:NC (1:1) or the mixture sample containing target:MM (1:1). HE% calculated according to the oxidation signals obtained after hybridization.

| | I (µA) | |
|---|---------------|------------|
| Probe-1 immobilized AuNPs/MoS₂-modified paper electrode | 28.39 ± 0.94 | HE% |
| miRNA-155 target | 19.74 ± 1.75 | 30.5 % |
| NC | 30.77 ± 8.37 | 8 % |
| MM | 22.52 ± 2.80 | 20.6 % |
| miRNA-155 target:NC (1:1) mixture | 20.59 ± 2.59 | 27.5 % |
| miRNA-155 target:MM (1:1) mixture | 21.23 ± 3.00 | 25.2 % |

Selectivity of the assay on voltammetric detection of miRNA-21 by AuNPs and MoS₂-modified paper electrode

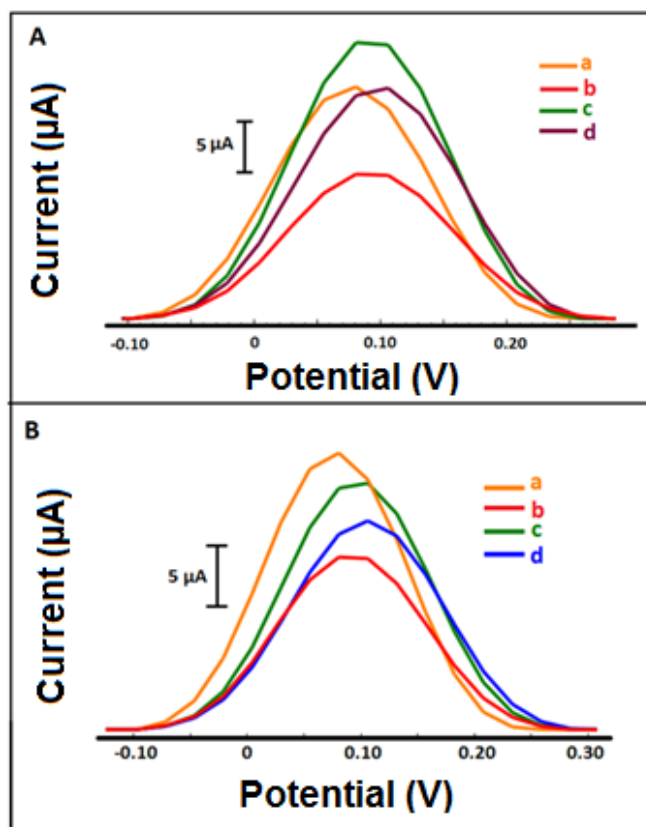


Figure S16. (A) Voltammograms representing the $[\text{Fe}(\text{CN})_6]^{3-/4-}$ oxidation signal obtained by (a) Probe-2 immobilized AuNPs/MoS₂-modified paper electrode in the absence of miRNA-21 target, after hybridization of Probe-2 with, (b) miRNA-21 target, (c) NC, and (d) MM, individually. (B) Voltammograms representing the $[\text{Fe}(\text{CN})_6]^{3-/4-}$ oxidation signal obtained by (a) Probe-2 immobilized AuNPs/MoS₂-modified paper electrode in the absence of miRNA-21 target, after hybridization of Probe-2 (b) with only miRNA-21 target, (c) target:NC (1:1) mixture, and (d) in target:MM (1:1) mixture.

Table S11. The average $[\text{Fe}(\text{CN})_6]^{3-/4-}$ oxidation signals (n=2) measured before and after hybridization of Probe-2 with miRNA-21 target, NC, MM, the mixture sample containing target:NC (1:1) or the mixture sample containing target:MM (1:1). HE% calculated according to the oxidation signals obtained after hybridization.

| | I (μA) | |
|---|---------------|------------|
| Probe-2 immobilized AuNPs/MoS₂-modified paper electrode | 23.06 ± 1.59 | HE% |
| miRNA-21 target | 16.20 ± 3.12 | 29 % |
| NC | 27.13 ± 3.01 | 17 % |
| MM | 24.54 ± 3.92 | 6 % |
| miRNA-21 target:NC (1:1) mixture | 21.66 ± 4.79 | 6 % |
| miRNA-21 target:MM (1:1) mixture | 21.88 ± 5.24 | 5 % |